High Dynamic Range Lensless THz Imaging Based on High-Average Power THz-TDS

S. Mansourzadeh[1], D. Damyanov[2], T. Vogel[1], M. Hoffmann[1], J. C. Balzer[2] and C.J. Saraceno[1]
[1] *Photonics and Ultrafast Laser Science, Ruhr University Bochum, 44801 Germany*
[2] *University of Duisburg-Essen, Duisburg, 47057 Germany*

***Abstract*— We demonstrate the potential of state-of-the-art high-average power THz-TDS for THz imaging applications, by performing lensless imaging of a 3D-printed mixed polymer probe using a migration algorithm. Images obtained with our 10-mW average power THz-TDS show a clear enhancement of dynamic range, which results in a significantly improved image contrast compared to the same measurements performed using a state-of-the-art commercial TDS system with less than 200-µW of average power. Our result is an important first step towards reflection-mode imaging of dielectric objects with an internal structure, potentially at long distances.**

I. INTRODUCTION

Terahertz (THz) radiation is attractive for sub-surface imaging applications due to a high penetration depth and good lateral resolution [1]. To-date, many imaging setups have been introduced using THz time-domain spectroscopy (THz-TDS), most often using THz time-of-flight technique [2]. With these technique, the temporal delay between reflected THz pulses provides the sample's internal structure [3]. This technique has been extensively exploited for example to analyze the layer structure of materials [4], in the biomedical application for histopathological imaging of cancerous tissue [5] or in hidden object detection in security application for looking through thin materials with low THz-absorption [6,7].

Despite many advantages, several difficulties have limited THz time-of-flight imaging to become extensive in the real-life scenarios. Typically, lenses or off-axis parabolic mirrors are used in the THz-TDS setup to collimate and re-focus the THz beam onto the sample to be imaged. Then the reflected beam is guided to the detector, resulting in two major difficulties: first a precise alignment of the optomechanics requires prior information about the position, orientation, and shape of the sample, which are usually unknown in real-life scenarios. Secondly the spot size of focused THz beam limits the lateral resolution and therefore, a sharp focusing is only achieved for limited depth of field.

A propitious method to overcome these difficulties has been introduced and evaluated by Damyanov et al. in [8,9]. The proposed imaging configuration is a lensless scheme based on radar migration image reconstruction that can generate high-resolution images of objects from the complete time-domain data regardless of their size, shape, orientation and relative position with respect to the THz emitter and detector, which represents an important advantage for realistic imaging scenarios. Since the technique is not limited by the spot size of the THz beam, the imaging of objects with subwavelength size is achievable due to the high lateral resolution. One important difficulty of this technique is that illumination is done with a typically low-average power divergent THz beam delivered by a commercial THz-TDS, resulting in extremely small reflected signal strength at the detector and minuscule signal-to-noise-ratio (SNR) figures, limiting the imaging capabilities especially for the detection of subsurface structures.

In this paper, we demonstrate that these difficulties can be overcome by using recently demonstrated state-of-the-art high-average power THz-sources for TDS [10]. We present a comparison between images taken with our high-average power (20-mW), home-built THz-TDS and a commercial THz-TDS system with less than 200-µW of average power, showing a large benefit in terms of image contrast.

II. EXPERIMENTAL SETUP AND RESULTS

A simplified scheme of the experimental setup is presented in Fig. 1. Our high average-power, few-cycle THz source is based on the same design as presented in [10]. The THz beam is generated based on optical rectification of a modelocked thin-disk laser using the tilted pulse front method in Lithium Niobate (LN). The crystal gets pumped with ultrashort pulses, delivered by a modelocked thin-disk laser. The oscillator delivers up to 100 W of average power at 13.4-MHz repetition rate. The pulses at this power level are 540 fs long with central wavelength of 1030 nm. Unlike many equivalent amplifier technologies, our oscillator delivers transform-limited, clean sech^2-shaped pulses and perfect beam quality.

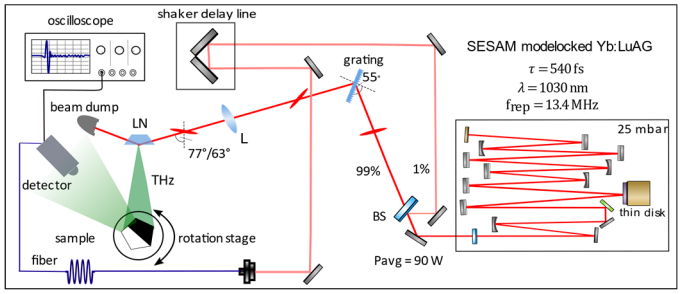

Fig. 1 Experimental setup, driving laser and high-average power THz-TDS with lensless imaging setup. The SESAM modeleocked oscillator is used to pump the LN crystal to generate high average-power THz. L: aspherical imaging lens, BS: beam splitter. In the imaging setup, the sample placed on a rotation stage reflects the divergent THz beam to the antenna.

We use this oscillator to generate THz pulses in a MgO-doped stoichiometric trapezoid LN crystal. A transmission grating is used to tilt the laser pulse front and afterward it is imaged to the LN crystal using an aspherical lens [10]. The generated THz beam is emitted perpendicularly to the front surface of the trapezoid. In this configuration, we routinely generate THz beam with average power up to 20 mW of THz power available for our imaging experiments. For the THz field detection, we use a fiber-coupled photoconductive antenna (PCA) from Fraunhofer Heinrich-Hertz-Institute, Berlin, Germany based on an InAlAs/InGaAs heterostructure [11]. The antenna has been designed to operate at a wavelength of 1550 nm. However, it can also operate with a 1030 nm laser probe beam. In our experiment, we use 5 mW of probe power coupled into the antenna. The output of the antenna is connected to a low noise

transimpedance amplifier with switchable gain up to 1×10^8 and bandwidth up to 200 MHz.

In our experiment, a pentagonal cross section sample with two different types of polymers glued to each other is used for imaging. The sample is scanned for full 360° with both systems. In order to get a full 2D rotational scan, the sample is placed on a rotation stage. The stage is rotated in steps of 1° and 360 measurements are performed. A high resolution 10-bit oscilloscope with a sampling rate of 200 kS/s is used for data acquisition. In the probe arm, the time delay is realized with a shaker with a scanning frequency of 1.5 Hz and a travel range of 330 ps and which can support the temporal shift of the reflected THz pulse from the sample with an 18 mm edge length.

In order to benchmark the performance of our system, we measured the same object using a commercial TDS (Tera-K15 from Menlo Systems). We imaged the same object with the commercial system and our high-power setup using the same number of averaged THz traces to average and the same antenna configuration. The resulting images from both systems are shown in Fig. 2. The x-axis and y-axis indicate the position of the sample and the z-axis shows the normalized reconstructed amplitude from measured data from the two systems.

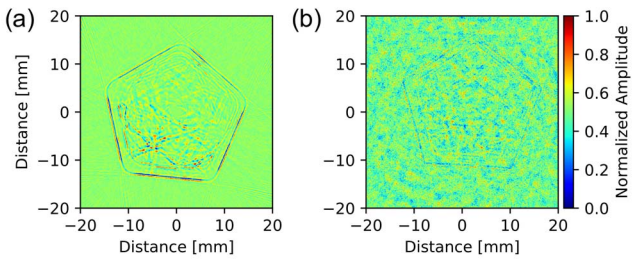

Fig. 2 Retrieved image of the pentagonal object, (a) using high power homebuilt THz-TDS setup and (b) Menlo System THz-TDS setup.

The figures demonstrate the enhanced imaging capabilities of the high-power system. The contour of the target is clearly reconstructed, where in the case of the commercial system the target is lost in the noise level. Furthermore, the inner structure of the sample is visible with the high-power system. In terms of image contrast, an 5 mm × 5 mm area next to the image is selected to calculate the standard deviation (SD) of the noise floor. The maximum amplitude is divided by the SD. The calculated value for high-power and commercial system are 26.7 and 5.1, respectively which shows the large enhancement in image contrast for the high-power system.

III. Summary

As a conclusion, we presented the potential of state-of-the-art high-average power THz-TDS operating in high-repetition rate regime for THz imaging applications, by performing lensless imaging of a 3D-printed mixed polymer object. To retrieve the image of the sample in this technique, a migration algorithm is used, which can reconstruct the image of the object without limiting us to have a priori information about the shape and position of the object. Although, for these experiments we do not considered the material characterization of the dielectric object, THz-TDS traces have the potential to extract material signatures. With the help of machine learning algorithms, this can be exploited to identify material in the near future.

Images obtained with our 20-mW average power THz-TDS shows a clear enhancement of dynamic range, which results in a significantly improved image contrast compared to the same measurements performed using a state-of-the-art commercial TDS system with less than 200-µW of average power.

IV. Acknowledgements

Diese Arbeit wurde unterstützt von der Deutschen Forschungsgemeinschaft (DFG, German Research Foundation) Projekt-ID 287022738 TRR 196, Projekte C10 und M05, und im Rahmen der Exzellenzstrategie des Bundes und der Länder – EXC 2033 – Projektnummer 390677874 – RESOLV. Sowie von der Alexander von Humboldt Stiftung (Sofja Kovalevskaja Preis, gestiftet vom Bundesministerium für Bildung und Forschung).

References

1. F. Ellrich, M. Bauer, N. Schreiner, A. Keil, T. Pfeiffer, J. Klier, S. Weber, J. Jonuscheit, F. Friederich, and D. Molter, "Terahertz Quality Inspection for Automotive and Aviation Industries," J. Infrared Millim. Terahertz Waves (2019).
2. E. Bründermann, H.-W. Hübers, and M. F. Kimmitt, *Terahertz Techniques* (Springer, 2012).
3. H. Guerboukha, K. Nallappan, and M. Skorobogatiy, "Toward real-time terahertz imaging," Adv. Opt. Photonics **10**(4), 843–938 (2018).
4. E.-M. Stübling, A. Rehn, T. Siebrecht, Y. Bauckhage, L. Öhrström, P. Eppenberger, J. C. Balzer, F. Rühli, and M. Koch, "Application of a robotic THz imaging system for sub-surface analysis of ancient human remains," Sci. Rep. **9**(1), 3390 (2019).
5. A. D'Arco, M. D. Di Fabrizio, V. Dolci, M. Petrarca, and S. Lupi, "THz Pulsed Imaging in Biomedical Applications," Condens. Matter **5**(2), 25 (2020).
6. M. Kowalski, "Hidden Object Detection and Recognition in Passive Terahertz and Mid-wavelength Infrared," J. Infrared Millim. Terahertz Waves **40**(11–12), 1074–1091 (2019).
7. Z. Ou, J. Wu, H. Geng, X. Deng, and X. Zheng, "Confocal terahertz SAR imaging of hidden objects through rough-surface scattering," Opt. Express **28**(8), 12405 (2020).
8. D. Damyanov, I. Willms, J. C. Balzer, B. Friederich, M. Yahyapour, N. Vieweg, A. Deninger, K. Kolpatzeck, X. Liu, A. Czylwik, and T. Schultze, "High Resolution Lensless Terahertz Imaging and Ranging," IEEE Access **7**, 147704–147712 (2019).
9. D. Damyanov, A. Batra, B. Friederich, T. Kaiser, T. Schultze, and J. C. Balzer, "High-Resolution Long-Range THz Imaging for Tunable Continuous-Wave Systems," IEEE Access **8**, 151997–152007 (2020).
10. F. Meyer, T. Vogel, S. Ahmed, and C. Saraceno, "Single-cycle, MHz-repetition rate THz source with 66 mW of average power," Opt. Lett. **45**(8), (2020).
11. R. J. B. Dietz, B. Globisch, M. Gerhard, A. Velauthapillai, D. Stanze, H. Roehle, M. Koch, T. Göbel, and M. Schell, "64 µW pulsed terahertz emission from growth optimized InGaAs/InAlAs heterostructures with separated photoconductive and trapping regions," Appl. Phys. Lett. **103**(6), 061103 (2013).